Mechanism of HN-3 cell apoptosis induced by carboplatin: Combination of mitochondrial pathway associated with Ca^{2+} and the nucleus pathways

BO SHEN[1*], WENJING MAO[2*], JIN-CHUL AHN[3,4], PHIL-SANG CHUNG[3,4] and PEIJIE HE[2]

[1]Institute of Radiation Medicine, Fudan University, Shanghai 200032;
[2]Department of Otolaryngology-Head and Neck Surgery, Shanghai Key Clinical Disciplines of Otorhinolaryngology, Eye and ENT Hospital of Fudan University, Shanghai 200031, P.R. China; [3]Department of Otolaryngology-Head and Neck Surgery; [4]Beckman Laser Institute Korea, Dankook University, Cheonan, Chungcheongnam 330-715, Republic of Korea

Abstract. Laryngeal carcinomas have been recognized as a serious health threat worldwide. In the present study, the mechanism of apoptosis in HN-3 cells induced by carboplatin (CBCDA), a widely used anti-cancer drug, was investigated. The pro-apoptotic effect of CBCDA in HN-3 cells was demonstrated to be time- and dose-dependent. Therefore, the stages of apoptosis were investigated in chronological order. The results demonstrated that excessive generation of cytosolic Ca^{2+} in HN-3 cells was initially triggered when cells were exposed to CBCDA, followed by the appearance of mitochondrial depolarization and oxidative stress, leading to the release of apoptosis-inducing factor. At later stages, expression of caspase-8 was increased due to the apoptotic signals originating from CBCDA-induced DNA damage, as well as caspase-9 and poly ADP ribose polymerase (PARP) expression upregulation. Glutathione decreased the available CBDCA concentration, decreased apoptosis and alleviating oxidative stress, thus reducing the actual effective concentration.

Correspondence to: Professor Peijie He, Department of Otolaryngology-Head and Neck Surgery, Shanghai Key Clinical Disciplines of Otorhinolaryngology, Eye and ENT Hospital of Fudan University, 83 Fenyang Road, Shanghai 200031, P.R. China
E-mail: hepj2002@sina.com

Professor Phil-Sang Chung, Department of Otolaryngology-Head and Neck Surgery, Dankook University, 329 Anseo-Dong, Cheonan, Chungcheongnam 330-715, Republic of Korea
E-mail: pschung@dankook.ac.kr

*Contributed equally

Abbreviations: CBDCA, carboplatin; GSH, glutathione; ROS, reactive oxygen species; MMP, mitochondrial membrane potential; MP, membrane potential; PARP, poly ADP ribose polymerase; AIF, poly ADP ribose polymerase

Key words: carboplatin, HN-3 cells, apoptosis, mitochondrial depolarization, glutathione

Mechanistic research may benefit the rational design of more efficient therapeutic strategies as well as development of novel platinum-based agents.

Introduction

Laryngeal carcinoma (LC), the second most common type of head and neck cancer, seriously threatens the health and longevity of individuals (1). Among all the subtypes of LC, laryngeal squamous cell carcinoma (LSCC) accounts for 95-98% of cases (1-3). Incidence of LSCC ranges from 3-10/100,000 in the USA alone and LSCC causes 2.1% of all cancer deaths worldwide, demonstrating that LSCC has become a worldwide public health problem (4,5). Beneath the complexity of every cancer lies a number of critical events that occur in the cell cycle that determine growth or shrinkage of the tumor. Apoptosis, which has an important role in chemotherapy, is a target of potent and specific therapeutics (6,7). Carboplatin (CBDCA) is a platinum-based agent that has been widely used in cancer chemotherapy. It is characterized by its ability to generate DNA lesions, thereby inhibiting replication and transcription, and finally leading to apoptosis (8,9). Specifically, CBDCA enters the cell by passive diffusion and undergoes hydrolysis to assume a form that interacts with nucleophilic purine bases in the DNA strand, resulting in major intra-strand cross linkages and minor inter-strand cross linkages. Subsequently, the cross linkages inhibit the process of DNA replication, causing errors in transcription (10-12). CBDCA was approved by the US Food and Drug Administration in the 1980s, and since then it has been regularly used in the treatment of several types of tumors (13).

Despite its extensive clinical application, the anticancer efficacy and safety of CBDCA remain important issues (14). The sensitivity of CBDCA therapy is a major obstacle to its successful clinical application (15,16). Due to the low incidence of side effects of CBDCA in clinical treatment, it is widely used in combination with other strategies (17,18). What may be inferred, therefore, is that understanding the factors and underlying mechanisms of cancer cell apoptosis during CBDCA treatment may provide valuable insight for the

rational design of more efficient therapeutic strategies, as well as development of novel platinum-based agents.

It has been widely recognized that apoptosis is initiated via two different routes: The death receptor pathway and the mitochondrial pathway (19-21). In the present study, the HN-3 cells were exposed to CBDCA to demonstrate the order of the occurrence of apoptotic phenomena, as well as mitochondrial activation, and the mechanism between them was investigated. In addition, it was reported that increased levels of glutathione (GSH), which is a reactive oxygen species (ROS) scavenger, may induce tumor cell resistance to CBDCA (22,23). Therefore, the effect of GSH on the mitochondrial activity and apoptosis of HN-3 cells was also investigated to extensively verify their roles in apoptosis.

Materials and methods

Cell culture. The laryngeal squamous cell carcinoma cell line HN-3 was kindly provided by the Asan Medical Center (Seoul, Korea). The cell line was cultured in RPMI-1640 medium (Hyclone; GE Healthcare Life Sciences, Logan, UT, USA) supplemented with 10% fetal bovine serum (Hyclone; GE Healthcare Life Sciences), penicillin (50 U/ml) and streptomycin (50 μg/ml) at 37˚C in a humidified incubator with 5% CO_2 and 95% air. CBDCA was obtained from Qilu Pharmaceutical Co., Ltd. (Jinan, China). GSH was purchased from Sigma-Aldrich (Merck KGaA, Darmstadt, Germany).

Cell viability assay. An MTT assay was used to measure cell viability. The cells were treated by CBDCA (0-5.0 mg/ml; 0-48 h) once 90% confluence was reached. Then the cells were incubated with 50 μl MTT solution (2 mg/ml) for 2 h. The MTT solution was exchanged with 100 μl dimethyl sulfoxide, shaken for 20 sec and the absorbance at 540 nm was measured. Cell viability was calculated according to the following equation: Cell viability (%)=(mean absorbance in treatment group/mean absorbance in control group) x100.

Hoechst 33342 and propidium iodide (PI) double staining. The concentration of GSH used was 5 mM. When the cells (5x10⁵ cells/well) were at 90% confluence, the samples were treated by carboplatin with or without GSH at 37˚C for 12 h. Following cultivation with CBDCA with or without GSH, cells were stained with Hoechst 33342/PI and observed by confocal microscopy as previously described (24). CBDCA-induced apoptosis was quantified according to the percentage of Hoechst 33342 and/or PI-positive stained cells by guavaSoft version 3.11 (EMD Millipore, Billerica, MA, USA).

Assessment of mitochondrial membrane potential (MMP). In brief, CBDCA-treated cells (the incubation began when the cell fusion degree was around 60%) cultured for 6 and 12 h, as well as the cells cultured with CBDCA and/or GSH for 12 h, were stained with rhodamine 123 (1 μM; Thermo Fisher Scientific, Inc., Waltham, MA, USA) for 30 min at 37˚C for observation by confocal microscopy, and further monitored using a flow cytometer (BD Biosciences, San Jose, CA, USA) and data were analyzed with the BD CellQuest Pro software version 2.0 (BD Biosciences) as described previously (25).

Detection of intracellular calcium. EGTA (2 mM) was added to chelate any residual Ca^{2+} in the RPMI-1640 medium. Cells were incubated with the Ca^{2+}-free medium and exposed to CBDCA (0.08 mg/ml) for 12 h at 37˚C, following which cells were incubated with 4 μM calcium Green-1 (Molecular Probes; Thermo Fisher Scientific, Inc.) for 30 min at 37˚C. Images of green calcium were collected with an LSM-510-META confocal microscope (Zeiss AG, Oberkochen, Germany) with an excitation wavelength of 488 nm, a 560-nm dichroic mirror, and a 505-550-nm band pass barrier filter. Quantification of calcium green-1 fluorescence was made by ImageJ version k1.45 (NIH, Bethesda, MD, USA). Intracellular Ca^{2+} was also monitored by flow cytometry following the same procedures described for rhodamine 123.

Western blot analysis. Antibodies against caspase-3 (cat. no. MAB4703), cleaved caspase-3 (cat. no. AB3623), caspase-8 (cat. no. MAB4708), poly ADP ribose polymerase (PARP; cat. no. AM30), cleaved PARP (AB3620) were purchased from Merck KGaA (Darmstadt, Germany); caspase-9 (cat. no. sc-8355) and apoptosis inducing factor (AIF; cat. no. sc-5586) antibodies were purchased from Santa Cruz Biotechnology, Inc. (Dallas, TX, USA); Antibodies against pro-caspase-3 (cat. no. ab32499), pro-caspase-12 (cat. no. ab8117), caspase-12 and cleaved-caspase-12 (cat. no. ab18766), GAPDH (cat. no. ab9485) was obtained from Abcam (Cambridge, UK); cytochrome *c* antibody (cat. no. 556433) was purchased from BD Biosciences. Horseradish peroxidase (HRP)-labeled goat anti-mouse (cat. no. A0216) and goat anti-rabbit immunoglobulin G (cat. no. A0208) secondary antibodies were purchased from Beyotime Institute of Biotechnology (Jiangsu, China).

Prior to protein extraction, cells were treated with CBDCA (0.04 or 0.08 mg/ml) with or without GSH (5 mM) for the indicated duration. Using RIPA lysis buffers (Sigma-Aldrich; Merck KGaA), total protein was extracted from HN-3 cells. Equivalent amounts of protein (100 μg/lane), whose concentration was determined by a BCA kit (Pierce; Thermo Fisher Scientific, Inc.), were loaded onto 10% polyacrylamide gels, subjected to electrophoresis, and transferred onto polyvinylidene fluoride membranes. Following blocking with 5% skim milk for 1 h at room temperature, primary antibodies were incubated overnight at 4˚C [cytochrome *c* (1:200); AIF (1:200); GAPDH (1:2,000); PARP (1:200); cleaved-PARP (1:200); caspase-3 (1:1,000); cleaved caspase-3 (1:1,000); pro-caspase-3 (1:1,000); caspase-9 (1:500); caspase-8 (1:500); caspase-12 (1:500); pro-caspase-12 (1:500)]. Each membrane was probed with horseradish peroxidase conjugated anti-mouse or anti-rabbit IgG antibody (1:1,000) for 1 h at room temperature. Labeled protein bands were visualized by an ECL + plus western blotting system kit (cat. no. RPN3352; GE Healthcare Life Sciences, Little Chalfont, UK) and were detected by a Kodak *in vivo* image analyzer (Kodak, Rochester, NY, USA). The bands were analyzed by densitometry using ImageJ version k1.45 (NIH, Bethesda, MD, USA).

Statistical analysis. Data are expressed as the mean ± standard deviation (n=3). The significance of differences was evaluated by one-way analysis of variance followed by the Least Significant Difference procedure by GraphPad Prism 6

software (GraphPad Software, Inc., La Jolla, CA, USA). P<0.05 was considered to indicate a statistically significant difference.

Results

The influence of CBDCA on HN-3 cells. The influence of CBDCA alone or in combination with GSH on HN-3 cells was initially investigated in terms of concentration and exposure duration.

The MTT assay results revealed that HN-3 cells exhibited various levels of cell viability, dependent on the concentration of CBDCA as well as the exposure time (Fig. 1). For each exposure duration, there was a minimal CBDCA concentration that resulted in a cell viability of ≤80%. Following 3 h exposure, this minimal concentration was ~5.00 mg/ml; following 6, 12, 24, 36 and 48 h, the minimal concentration was 2.50, 0.63, 0.16, 0.08 and 0.04 mg/ml, respectively. This revealed a downward trend in the concentration required as the exposure time increased.

The mode of cell death at each exposure duration, namely apoptosis and necrosis, was evaluated by Hoechst 33342/PI double staining following CBDCA and/or GSH treatment (Fig. 2). When exposed to 0.08 mg/ml CBDCA (Fig. 2A), apoptosis was initiated in a time-dependent manner; no obvious indication of apoptosis (<20%) was observed prior to 24 h of exposure. When HN-3 cells were exposed to various concentrations of CBDCA for 24 h, apoptosis/necrosis was concentration dependent (Fig. 2B). In the concentration range of 0 to 0.64 mg/ml, apoptosis was significantly increased as the concentration increased. At higher concentrations, a gradual increase in the proportion of necrotic cells, as well as a decrease in the proportion of apoptotic cells was observed. These results demonstrated that the influence of CBDCA on HN-3 cells was exerted in a dose and time-dependent manner.

In the confocal microscopy images (Fig. 2C), intact homogeneous blue nuclei were considered viable; condensed/fragmented blue nuclei were considered early apoptotic; condensed/fragmented pink nuclei were considered late apoptotic; and pink intact nuclei were considered necrotic. In the control group (no CBDCA or GSH treatment), intact homogeneous blue and round nuclei were observed. This was also observed in cells cultured with added GSH. Ubiquitous condensed/fragmented blue nuclei and pink nuclei were observed in the CBDCA treated group, whereas fewer pink nuclei were observed in cells exposed to CBDCA and GSH simultaneously. It can be inferred that CBDCA at a concentration of 0.08 mg/ml induced both early and late stage apoptosis following 24 h incubation, and the addition of GSH caused a decrease in the amount of late apoptotic cells.

Mitochondrial depolarization. An event now recognized to be important in apoptosis is the mitochondrial permeability transition (26,27). In the present study, the response of mitochondria in HN-3 cells exposed to CBDCA was investigated via staining methods and monitoring the MMP, as well as the membrane potential (MP), in a single cell by flow cytometry combined with the fluorescence detection of rhodamine 123. Under confocal microscopy, it was observed that the majority of bright fluorescent spheres became faint following exposure to CBDCA for 12 h (Fig. 3A), and MMP was noticeably shifted left (Fig. 3B).
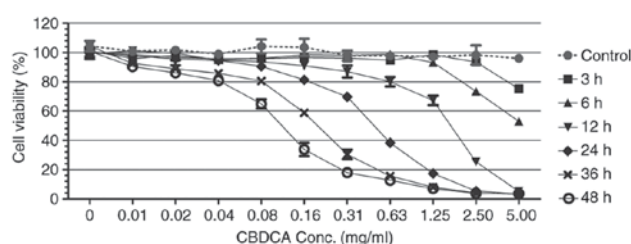

Figure 1. Effect of CBDCA treatment concentration and duration on HN-3 cell viability. CBDCA, carboplatin; conc, concentration.

Based on these results, it was concluded that mitochondrial depolarization occurred in HN-3 cells exposed to CBDCA for 12 h. However, when exposed to the mixture of CBDCA and GSH, the faintness and intensity of the sphere fluorescence, as well as the MMP value, were partially restored (Fig. 3C and D), indicating that mitochondrial depolarization was alleviated. No marked differences were observed in cells treated with CBCDA alone in comparison to cells treated with GSH alone (Fig. 3C).

Ca^{2+} is a universal signaling molecule that controls a variety of physiological functions, including those involving the mitochondria (28). In the present study, exposure to CBDCA alone induced a significant elevation of Ca^{2+} concentration in HN-3 cells (Fig. 4A). This increase was effectively inhibited by the addition of GSH, and no obvious impact on the intracellular Ca^{2+} level was observed when cells were exposed to GSH alone (Fig. 4A and B). Accordingly, the intracellular level of Ca^{2+} displayed a distinct rightward shift in the flow cytometry results (Fig. 4C), upon exposure to CBDCA, which was restored by the addition of GSH into the cell culture.

Activation of caspases and PARP. Mitochondria serve an important role in cell death through the release of pro-apoptotic factors, including cytochrome *c* and apoptosis-inducing factor (AIF), which activate caspase-dependent and caspase-independent cell death, respectively (29). As presented in Fig. 5A, the expression levels of cytochrome *c* and AIF were upregulated following exposure to CBDCA, particularly in the first 24 h. The decrease in cytochrome *c* and AIF expression observed following 24 h may have resulted from loss of mitochondrial function. To confirm the effects of CBDCA on apoptosis, apoptosis-associated protein expression was further evaluated (Fig. 5B). Western blot analysis revealed that there was a time-dependent increase in the expression of the downstream caspase cascade, including caspase-8/-9 and PARP. Increased expression of caspase-8 was observed following 12 h, and increased expression of caspase-9, cleaved caspase-3 and PARP was observed following ~36 h. These results were in accordance with the apoptosis results summarized above, confirming that apoptosis predominantly occurred when cells were exposed to CBDCA for a duration of >24 h. Caspase-8 may have been induced when Ca^{2+} and mitochondrial depolarization took effect after 12 h, and caspase-9 may have been induced by cytochrome *c* release after 36 h.

When the exposure time was fixed at 12 h, a comparison was made among the control and CBDCA and GSH treatment groups, alone or in combination. A weak dose dependent release of cytochrome *c* and AIF was detected (Fig. 6A). By contrast, there was a marked dose-dependent increase in the expression
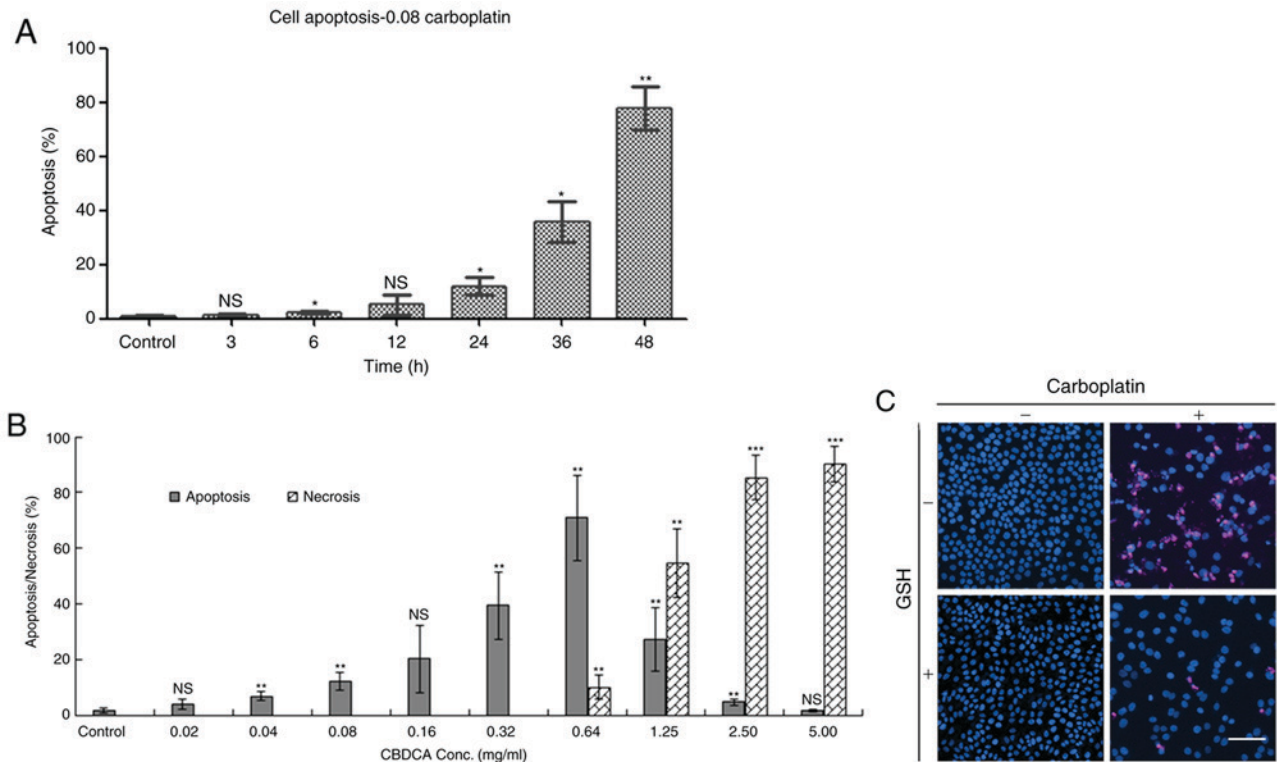
Figure 2. HN-3 cell apoptosis and necrosis following treatment with CBDCA. (A) Apoptosis over time when HN-3 cells were exposed to 0.08 mg/ml CBDCA. (B) Apoptosis and necrosis evaluation when HN-3 cells were exposed to increasing concentration of CBDCA for 24 h. (C) Confocal microscopy images from PI and Hoechst 33342 stained HN-3 cells treated with CBDCA and/or GSH for 24 h. CBDCA, carboplatin; GSH, glutathione; NS, not significant; conc, concentration. Scale bar=100 μm. Data were presented as the mean ± standard deviation. *P<0.05, **P<0.01, ***P<0.001 vs. control.
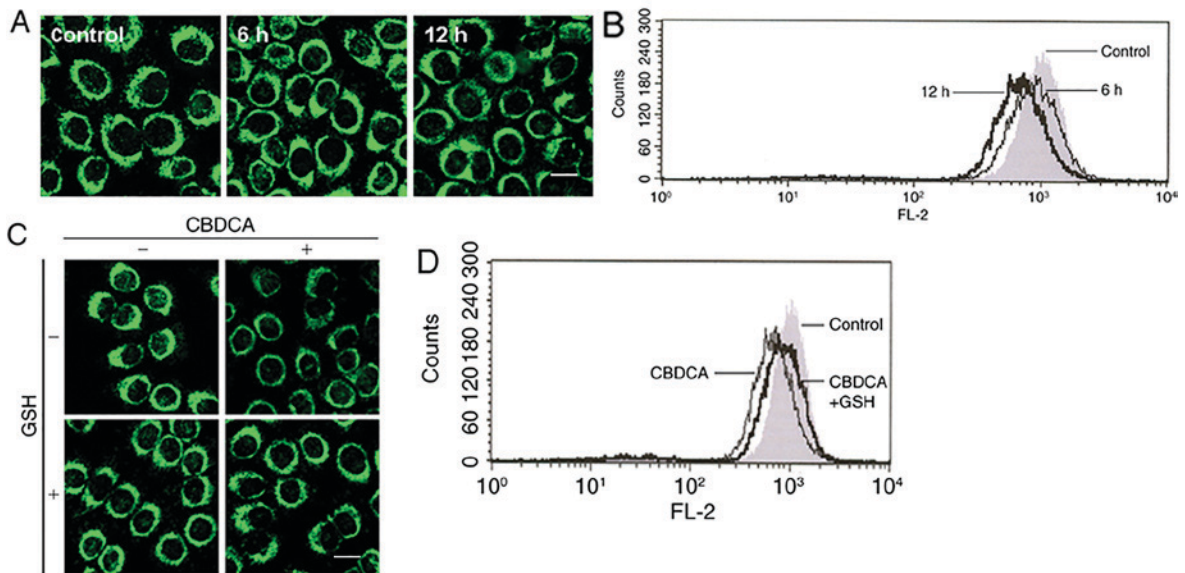

Figure 3. CBDCA induces MMP collapse in HN-3 cells. MMP was detected 6 and 12 h following CBDCA treatment with (A) confocal microscopy and (B) flow cytometry. CBDCA with or without GSH induced the MMP collapse in HN-3 cells. MMP was detected by (C) confocal microscopy and (D) flow cytometry. Scale bar=20 μm. CBDCA, carboplatin; GSH, glutathione; MMP, mitochondrial membrane potential.

of caspase-12/-8/-9/-3 and cleaved PARP (Fig. 6B). Upregulation of apoptosis-associated protein expression was observed in the group treated with 0.08 mg/ml CBDCA alone, but this was less evident when the CBDCA concentration was 0.04 mg/ml. Furthermore, treatment with CBDCA and GSH almost entirely inhibited the activating effects of CBDCA at 0.08 mg/ml.

These data indicated that the activation of apoptosis-associated proteins was sensitive to the concentration of CBDCA. Fig. 7 demonstrates that apoptosis predominantly occurred through two signal-transduction pathways: The death receptor pathway and the mitochondrial pathway, which are also termed the extrinsic and intrinsic apoptotic pathways, respectively.
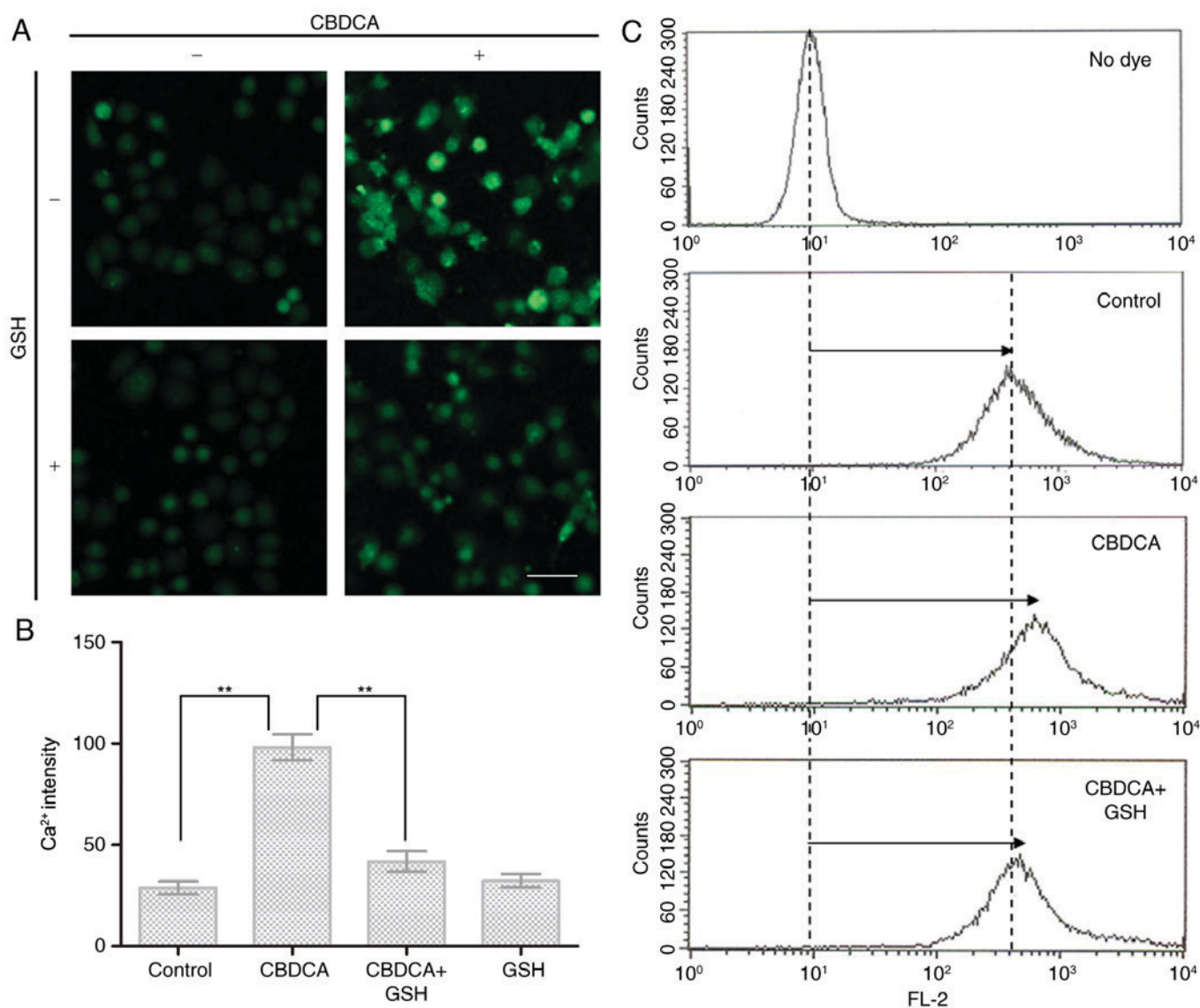
Figure 4. Intracellular Ca^{2+} levels in response to CBDCA treatment with or without GSH. Ca^{2+} levels were monitored by (A) confocal microscopy and (B) flow cytometry. (C) Quantification of calcium green-1 fluorescence by ImageJ. CBDCA, carboplatin; GSH, glutathione. Scale bar=50 μm. Data were presented as the mean ± standard deviation. **P<0.01.

Discussion

As an anti-cancer drug, CBDCA was demonstrated to inhibit cell viability and have an apoptosis-inducing effect in the present study. Cell viability was notably suppressed by CBDCA but was protected by the addition of GSH. These effects were dose- and time-dependent.

The mitochondrial pathway of apoptosis is initiated by death-inducing stimuli including oxidative stress and UV radiation, which leads to the activation of caspase-9 through the mitochondria (30,31). Extrinsic apoptosis initiated by death-inducing stimuli involves the complex formation of death-domain-containing-proteins and consequent activation of caspase-8. In addition, in the presence of death-inducing stimuli, the endoplasmic reticulum may also initiate apoptosis via the activation of caspase-12 (20,21,32). As for the death-inducing stimuli mentioned above, there is increasing evidence to support the theory that the major mechanism of cell apoptosis induced by CBDCA includes direct covalent

binding between CBDCA and DNA, to form DNA adducts, as well as oxidative stress due to ROS generation (33,34). These results indicate that CBDCA-induced apoptosis is mediated through the mitochondrial pathway (8,35). In the present study, the protective effect of GSH indicated that ROS served a causative role. Regarding endoplasmic reticulum-related apoptosis initiation, the death-inducing stimulus generated may have been excessive Ca^{2+}, as demonstrated by the significant increase in Ca^{2+} in response to CBDA detected in the present study, as well as in previous research (16).

When HN-3 cells were exposed to CBDCA in sufficient concentrations, the agent successfully crossed the cell membrane, underwent hydrolysis and became positively charged. The current experimental results revealed that when exposed to CBDCA for 12 h, by which time apoptosis was, although not significant, notably increased, the HN-3 cells had enhanced MP and increased intracellular Ca^{2+} concentration, as well as mitochondrial depolarization. Upregulated expression of caspase-8 was observed when cells were
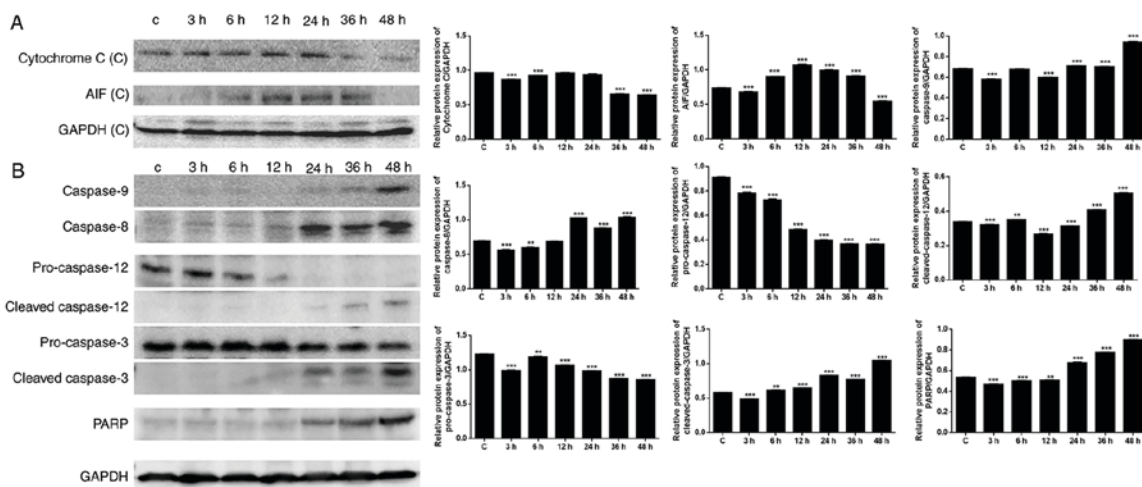
Figure 5. Expression of apoptosis-associated proteins following CBDCA treatment. (A) Expression of cytochrome *c* and AIF when cells were exposed to CBDCA. (B) Expression of caspase-8, -9, PARP, pro-caspase-3, -12, cleaved caspase-3 and -12. GAPDH was included as a loading control. CBDCA, carboplatin; PARP, poly ADP ribose polymerase; AIF, apoptosis inducing factor. Data were presented as the mean ± standard deviation. **$P < 0.01$, ***$P < 0.001$ vs. Control.
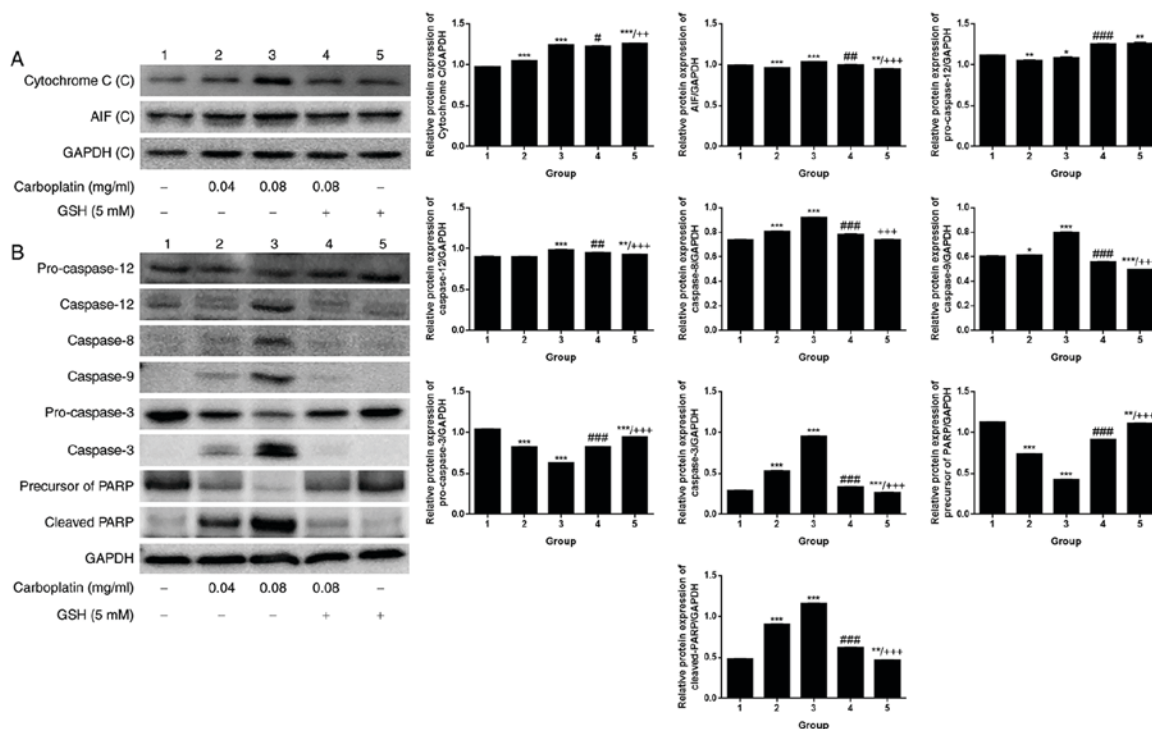

Figure 6. Expression of apoptosis-associated proteins following CBDCA treatment with or without GSH. (A) Cytochrome *c* and AIF expression, as well the (B) expression of caspase-3, -8, -9, -12, cleaved PARP, pro-caspase-3 and -12 following treatment with CBDCA, GSH or a combination for 12 h. GAPDH was included as a loading control. GSH, glutathione; CBDCA, carboplatin; PARP, poly ADP ribose polymerase; AIF, apoptosis inducing factor. Data were presented as the mean ± standard deviation. *$P < 0.05$, **$P < 0.01$, ***$P < 0.001$ vs. group 1. #$P < 0.05$, ##$P < 0.01$, ###$P < 0.001$ vs. group 3. ++$P < 0.01$, +++$P < 0.001$ vs. group 4.

exposed to CBDCA for 24 h (12 h following Ca^{2+} overload and mitochondrial depolarization). PARP took effect at a later stage, after cells were exposed to CBDCA for ~36 h, and caspase-9 was activated last, when cells were exposed to CBDCA for ~48 h.

After 12 h, the activated apoptotic signaling molecules were released into the cytoplasm, which contains many pro-apoptotic factors such as cytochrome *c*, AIF and pro-caspase-9 in the intermembrane space (28,36,37). In addition, mitochondrial depolarization was almost fully restored by the addition of GSH, which is an ROS scavenger. Oxidative stress during apoptosis is thought to be associated with the malfunction of the mitochondrial respiratory chain and disengagement of cytochrome *c*, as well as alteration in mitochondrial transmembrane potential and membrane permeability (38,39). Therefore, it can be inferred that the release of AIF is responsible for the enhanced ROS and oxidative stress. Oxidative stress may have induced mitochondrial
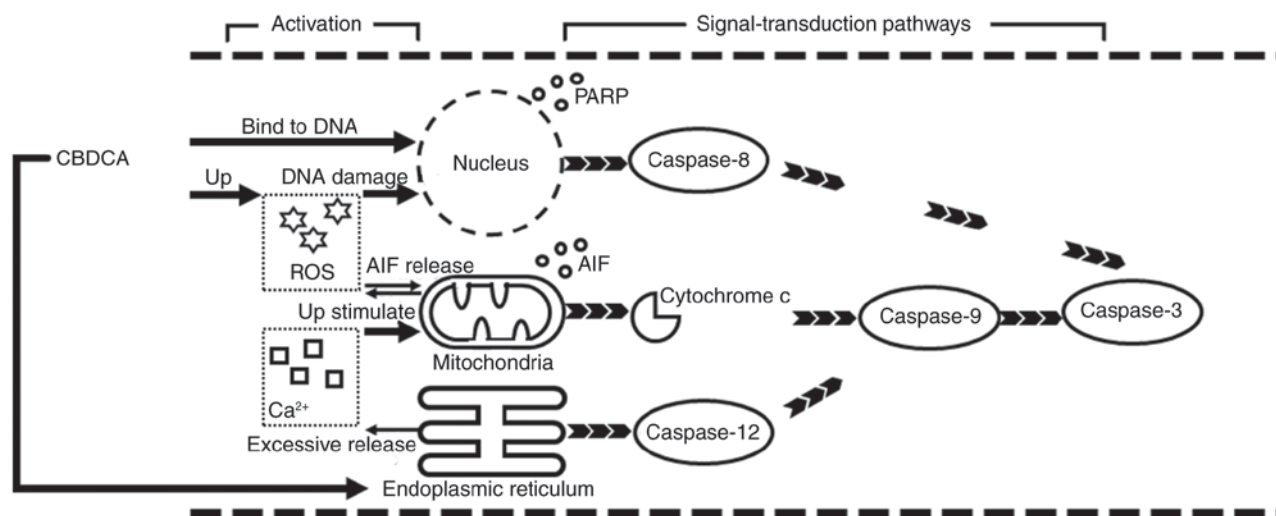
Figure 7. Schematic illustrating CBDCA-mediated cell apoptosis over time. CBDCA promoted the occurrence of mitochondrial depolarization and Ca^{2+} overload, leading to cytochrome c release and subsequent caspase-9 activation. CBDCA, carboplatin; AIF, apoptosis inducing factor; PARP, poly ADP ribose polymerase; ROS, reactive oxygen species.

permeability transition, which leads to the release of AIF. Furthermore, the mitochondrial permeability transition may have generated more ROS from the mitochondria in a positive feedback loop.

In the present study, simultaneous with AIF release (at ~12 h), an increase in the amount of Ca^{2+} was detected. The occurrence of MP excluded the possibility that CBDCA directly destroyed the membrane function of the cells. Instead, membrane polarization suggested that HN-3 cells were processing the excessive intracellular Ca^{2+} by increasing membrane polarization to inhibit Ca^{2+} influx. Oxidative stress has been reported to be induced by increased intracellular Ca^{2+} (40). Excessive cytosolic Ca^{2+} induced by exposure to CBDCA in HN-3 cells is transferred to the mitochondria by the endoplasmic reticulum (28). This may have led to alterations in ultra-structural integrity and a reduction in the MMP in the present study. CBDCA may increase Ca^{2+} release from the endoplasmic reticulum, leading to the production of nitric oxide (NO). Mitochondrial uptake of Ca^{2+} and peroxynitrite, which is generated from the interaction of NO and superoxide anion, block mitochondrial respiration resulting in the generation of ROS (29). However, although oxidative stress is induced by Ca^{2+}, this excessive release of Ca^{2+} is effectively inhibited by the addition of GSH. This is because the high level of GSH effectively 'mops up' the activated platinum in the cytoplasm by direct binding prior to its interaction with the organelles. This causes a loss of the effectiveness of CBDCA to induce additional Ca^{2+} release (22). This CBDCA-induced excessive intracellular Ca^{2+} release is sufficient to act as a death-inducing stimulus, which results in early and persistent mitochondrial depolarization with perturbation or rupture of the outer mitochondrial membrane, as well as induced oxidative stress and AIF release. In the present study, excessive Ca^{2+}-induced AIF release occurred at the earliest stage (the first 12 h) of CBDCA treatment, but did not persist due to mitochondrial damage, which ceased functioning following 36 h of CBDCA exposure. Therefore, AIF release was likely not the main mechanism of apoptosis.

With prolonged exposure to CBDCA, a variety of interactions took effect in coordination with cytochrome c, caspase-8 and PARP. The apoptotic signals triggered caspase activation by either activating initiator caspases, including caspase-8, or through the release of caspase-activating factors, including cytochrome c and AIF from the mitochondria. In addition, cell death occurred not only through the caspases, but also through a PARP-mediated cell death pathway, causing AIF to translocate from the mitochondria into the nucleus. Furthermore, it has been reported that CBDCA molecule could interact with DNA molecules (33). The linkage between DNA and CBDCA may be the most cytotoxic effect, through inhibiting the process of DNA replication, causing errors in replication and inducing the signaling molecules of apoptosis (41). These activities triggered caspase-8 activation or the PARP-mediated cell death pathway.

The existence of different stages of apoptosis and the fact that apoptosis-associated factors were activated at different times accounted for the time-dependent response of HN-3 cells treated with CBDCA. For example, the CBDCA required a synergistic effect of caspase-8 and -9, as well as the PARP pathway to exert its full effectiveness. The present study also suggested that CBDCA-induced apoptosis in HN-3 cells is concentration dependent. The dose-dependence of CBDCA may be due to the DNA repair machinery, which is activated when mild damage occurs but under severe insult that results in extensive DNA damage, caspase induction occurs over the activation of DNA repair (37).

In conclusion, CBDCA exerted a time- and dose-dependent inhibitory effect in HN-3 cells in the present study. The results demonstrated the involvement of mitochondria at the initiation of apoptosis triggered by excessive intracellular Ca^{2+}. Investigation of the expression of apoptosis-associated proteins revealed that mitochondria act as an independent upstream mediator of the CBDCA-induced apoptosis pathways, cooperating with the nuclear pathways that take effect earlier than the mitochondrial pathways. The present findings may have useful implications for the rational design of more

efficient therapeutic strategies as well as the development of novel platinum-based agents.

Acknowledgements

Not applicable.

Funding

Availability of data and materials

The datasets used and/or analyzed during the current study are available from the corresponding author on reasonable request.

Authors' contributions

PH and PC made substantial contributions to the concept and design of the present study, and the examination of the manuscript. BS and WM conducted experiments and produced the manuscript. JA conducted experiments and analyze the experimental data.

Ethics approval and consent to participate

Not applicable.

Patient consent for publication

Not applicable.

Competing interests

The authors declare that they have no competing interests.

References

1. Zhang W, Yan Y, Gu M, Wang X, Zhu H, Zhang S and Wang W: High expression levels of Wnt5a and Ror2 in laryngeal squamous cell carcinoma are associated with poor prognosis. Oncol Lett 14: 2232-2238, 2017.
2. Riga M, Chelis L, Danielides V, Vogiatzaki T, Pantazis TL and Pantazis D: Systematic review on T3 laryngeal squamous cell carcinoma; still far from a consensus on the optimal organ preserving treatment. Eur J Surg Oncol 43: 20-31, 2017.
3. Shen Z, Cao B, Lin L, Zhou C, Ye D, Qiu S, Li Q and Cui X: The clinical signification of claudin-11 promoter hypermethylation for laryngeal squamous cell carcinoma. Med Sci Monit 23: 3635-3640, 2017.
4. Siegel R, Ma J, Zou Z and Jemal A: Cancer statistics, 2014. CA Cancer J Clin 64: 9-29, 2014.
5. Mao Y, Zhang DW, Lin H, Xiong L, Liu Y, Li QD, Ma J, Cao Q, Chen RJ, Zhu J and Feng ZQ: Alpha B-crystallin is a new prognostic marker for laryngeal squamous cell carcinoma. J Exp Clin Cancer Res 31: 101, 2012.
6. Evan GI and Vousden KH: Proliferation, cell cycle and apoptosis in cancer. Nature 411: 342-348, 2001.
7. Radogna F, Dicato M and Diederich M: Cancer-type-specific crosstalk between autophagy, necroptosis and apoptosis as a pharmacological target. Biochem Pharmacol 94: 1-11, 2015.
8. Sousa GFD, Wlodarczyk SR and Monteiro G: Carboplatin: Molecular mechanisms of action associated with chemoresistance. Braz J Pharm Sci 50: 693-701, 2014.
9. Castrellon AB, Pidhorecky I, Valero V and Raez LE: The role of carboplatin in the neoadjuvant chemotherapy treatment of triple negative breast cancer. Oncol Rev 11: 324, 2017.
10. Johnstone TC, Park GY and Lippard SJ: Understanding and improving platinum anticancer drugs-phenanthriplatin. Anticancer Res 34: 471-476, 2014.
11. Fong CW: Platinum based radiochemotherapies: Free radical mechanisms and radiotherapy sensitizers. Free Radic Biol Med 99: 99-109, 2016.
12. Lee CK, Jung M, Choi HJ, Kim HR, Kim HS, Roh MR2, Ahn JB, Chung HC, Heo SJ, Rha SY and Shin SJ: Results of a phase II study to evaluate the efficacy of docetaxel and carboplatin in metastatic malignant melanoma patients who failed first-line therapy containing dacarbazine. Cancer Res Treat 47: 781-789, 2015.
13. Sanborn RE: Cisplatin versus carboplatin in NSCLC: Is there one 'best' answer? Curr Treat Option On 9: 326-342, 2008.
14. Comella P, Gambardella A, Frasci G, Avallone A and Costanzo R; SICOG investigators: Comparison of the safety and efficacy of paclitaxel plus gemcitabine combination in young and elderly patients with locally advanced or metastatic non-small cell lung cancer. A retrospective analysis of the Southern Italy Cooperative Oncology Group trials. Crit Rev Oncol Hematol 65: 164-171, 2008.
15. Barghout SH, Zepeda N, Vincent K, Azad AK, Xu Z, Yang C, Steed H, Postovit LM and Fu YX: RUNX3 contributes to carboplatin resistance in epithelial ovarian cancer cells. Gynecol Oncol 138: 647-655, 2015.
16. Lum E, Vigliotti M, Banerjee N, Cutter N, Wrzeszczynski KO, Khan S, Kamalakaran S, Levine DA, Dimitrova N and Lucito R: Loss of DOK2 induces carboplatin resistance in ovarian cancer via suppression of apoptosis. Gynecol Oncol 130: 369-376, 2013.
17. de Castria TB, da Silva EM, Gois AF and Riera R: Cisplatin versus carboplatin in combination with third-generation drugs for advanced non-small cell lung cancer. Cochrane Db Syst Rev 8: CD009256, 2013.
18. Zhang Q, Cheng Y, Huang L, Bai Y, Liang J and Li X: Inhibitory effect of carboplatin in combination with bevacizumab on human retinoblastoma in an in vitro and in vivo model. Oncol Lett 14: 5326-5332, 2017.
19. Montero AJ and Jassem J: Cellular redox pathways as a therapeutic target in the treatment of cancer. Drugs 71: 1385-1396, 2011.
20. Fulda S and Debatin KM: Extrinsic versus intrinsic apoptosis pathways in anticancer chemotherapy. Oncogene 25: 4798-4811, 2006.
21. Green DR: Apoptotic pathways: Paper wraps stone blunts scissors. Cell 102: 1-4, 2000.
22. Kelland L: The resurgence of platinum-based cancer chemotherapy. Nat Rev Cancer 7: 573-584, 2007.
23. Nicolson MC, Orr RM, O'Neill CF and Harrap KR: The role of platinum uptake and glutathione levels in L1210 cells sensitive and resistant to cisplatin, tetraplatin or carboplatin. Neoplasma 39: 189-195, 1992.
24. He P, Ahn JC, Shin JI, Hwang HJ, Kang JW, Lee SJ and Chung PS: Enhanced apoptotic effect of combined modality of 9-hydroxypheophorbide alpha-mediated photodynamic therapy and carboplatin on AMC-HN-3 human head and neck cancer cells. Oncol Rep 21: 329-334, 2009.
25. He P, Bo S, Chung PS, Ahn JC and Zhou L: Photosensitizer effect of 9-hydroxypheophorbide α on diode laser-irradiated laryngeal cancer cells: Oxidative stress-directed cell death and migration suppression. Oncol Lett 12: 1889-1895, 2016.
26. Evtodienko YuV, Teplova V, Khawaja J and Saris NE: The Ca(2+)-induced permeability transition pore is involved in Ca(2+)-induced mitochondrial oscillations: A study on permeabilised Ehrlich ascites tumour cells. Cell Calcium 15: 143-152, 1994.
27. Hunter DR and Haworth RA: The Ca2+-induced membrane transition in mitochondria. I. The protective mechanisms. Arch Biochem Biophys 195: 453-459, 1979.
28. Giorgi C, Romagnoli A, Pinton P and Rizzuto R: Ca2+ signaling, mitochondria and cell death. Curr Mol Med 8: 119-130, 2008.

29. Hong SJ, Dawson TM and Dawson VL: Nuclear and mitochondrial conversations in cell death: PARP-1 and AIF signaling. Trends Pharmacol Sci 25: 259-264, 2004.
30. Gonzalez D, Bejarano I, Barriga C, Rodriguez AB and Pariente JA: Oxidative stress-induced caspases are regulated in human myeloid HL-60 cells by calcium signal. Curr Signal Transduct Ther 5: 181-186, 2010.
31. Wajant H: The Fas signaling pathway: More than a paradigm. Science 296: 1635-1636, 2002.
32. Su SH, Su SJ, Lin SR and Chang KL: Cardiotoxin-III selectively enhances activation-induced apoptosis of human CD8+ T lymphocytes. Toxicol Appl Pharmacol 193: 97-105, 2003.
33. Hah SS, Stivers KM, de Vere White RW and Henderson PT: Kinetics of carboplatin-DNA binding in genomic DNA and bladder cancer cells as determined by accelerator mass spectrometry. Chem Res Toxicol 19: 622-626, 2006.
34. Cheng CF, Juan SH, Chen JJ, Chao YC, Chen HH, Lian WS, Lu CY, Chang CI, Chiu TH and Lin H: Pravastatin attenuates carboplatin-induced cardiotoxicity via inhibition of oxidative stress associated apoptosis. Apoptosis 13: 883-894, 2008.
35. Hwang H, Biswas R, Chung PS and Ahn JC: Modulation of EGFR and ROS induced cytochrome c release by combination of photodynamic therapy and carboplatin in human cultured head and neck cancer cells and tumor xenograft in nude mice. J Photochem Photobiol B 128: 70-77, 2013.
36. Gunter TE and Pfeiffer DR: Mechanisms by which mitochondria transport calcium. Am J Physiol 258: C755-C786, 1990.
37. Joza N, Susin SA, Daugas E, Stanford WL, Cho SK, Li CY, Sasaki T, Elia AJ, Cheng HY, Ravagnan L, et al: Essential role of the mitochondrial apoptosis-inducing factor in programmed cell death. Nature 410: 549-554, 2001.
38. Zamzami N, Marchetti P, Castedo M, Decaudin D, Macho A, Hirsch T, Susin SA, Petit PX, Mignotte B and Kroemer G: Sequential reduction of mitochondrial transmembrane potential and generation of reactive oxygen species in early programmed cell death. J Exp Med 182: 367-377, 1995.
39. Boya P, Morales MC, Gonzalez-Polo RA, Andreau K, Gourdier I, Perfettini JL, Larochette N, Deniaud A, Baran-Marszak F, Fagard R, et al: The chemopreventive agent N-(4-hydroxyphenyl) retinamide induces apoptosis through a mitochondrial pathway regulated by proteins from the Bcl-2 family. Oncogene 22: 6220-6230, 2003.
40. Richter C and Kass GE: Oxidative stress in mitochondria: Its relationship to cellular Ca2+ homeostasis, cell death, proliferation, and differentiation. Chem Biol Interact 77: 1-23, 1991.
41. Los G, Smals OA, van Vugt MJ, van der Vlist M, den Engelse L, McVie JG and Pinedo HM: A rationale for carboplatin treatment and abdominal hyperthermia in cancers restricted to the peritoneal cavity. Cancer Res 52: 1252-1258, 1992.